

Supporting Information

Effects of Aluminum Substitution in Nickel-rich Layered $\text{LiNi}_x\text{Al}_{1-x}\text{O}_2$ ($x=0.92, 0.95$) Positive Electrode Materials for Li-Ion Batteries on High-Rate Cycle Performance

Received 00th January 20xx,
Accepted 00th January 20xx

DOI: 10.1039/x0xx00000x

Haruki Kaneda,^{*ab} Yuki Furuichi,^a Atsunori Ikezawa^b and Hajime Arai^{*b}

a. Sumitomo Metal Mining Co., Ltd, Battery Research Laboratories

17-3 Isoura-cho, Niihama, Ehime 792-0002, Japan. E-mail: haruki.kaneda.d3@smm-g.com

b. School of Materials Science and Technology, Tokyo Institute of Technology

4259 Nagatusta-cho, Midori-ku, Yokohama Kanagawa 226-8502, Japan. E-mail: arai.h.af@m.titech.ac.jp

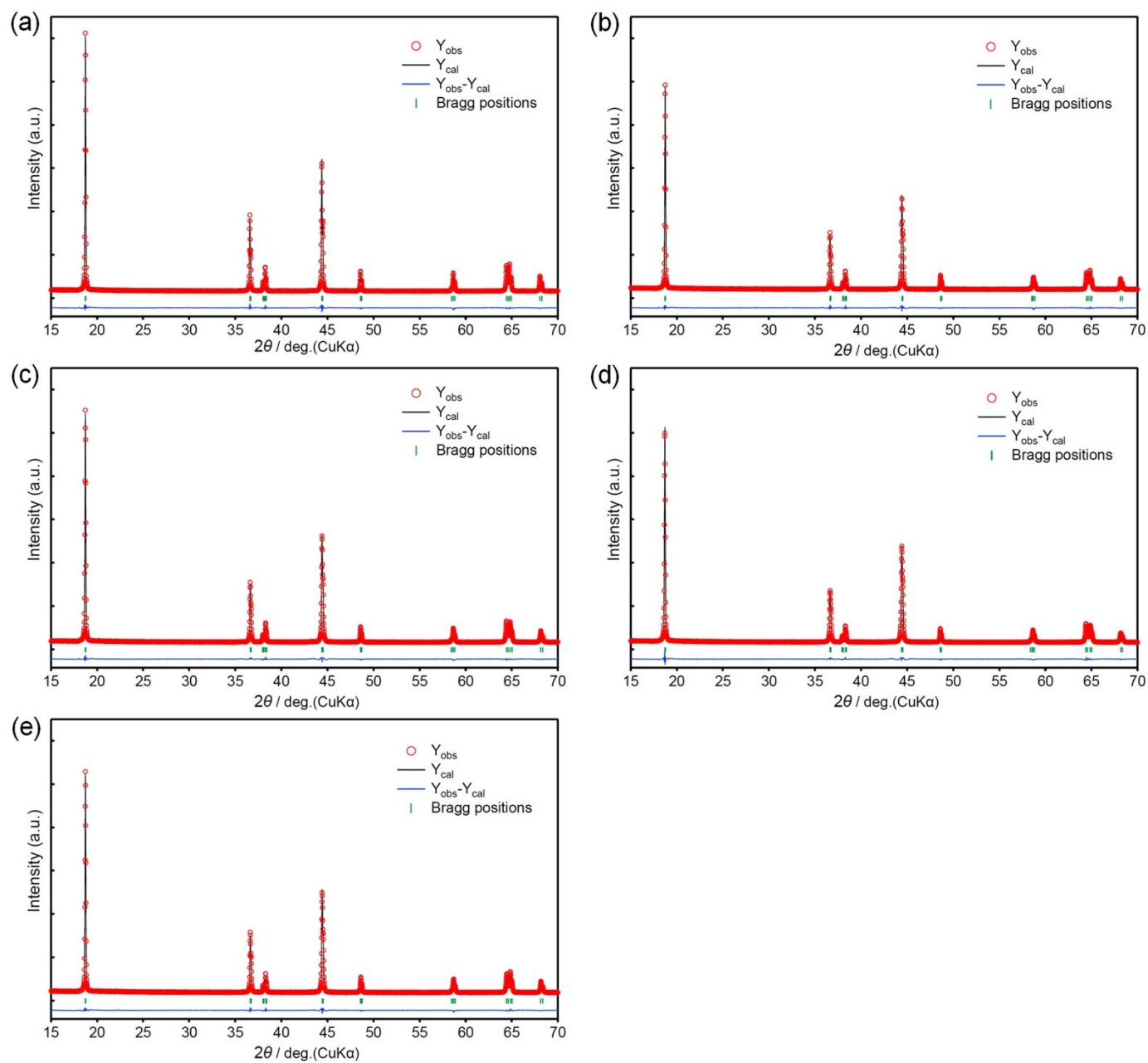


Figure S1 XRD patterns of (a) LNO, (b) NC95, (c) NA95, (d) NA92, (e) NCA95.

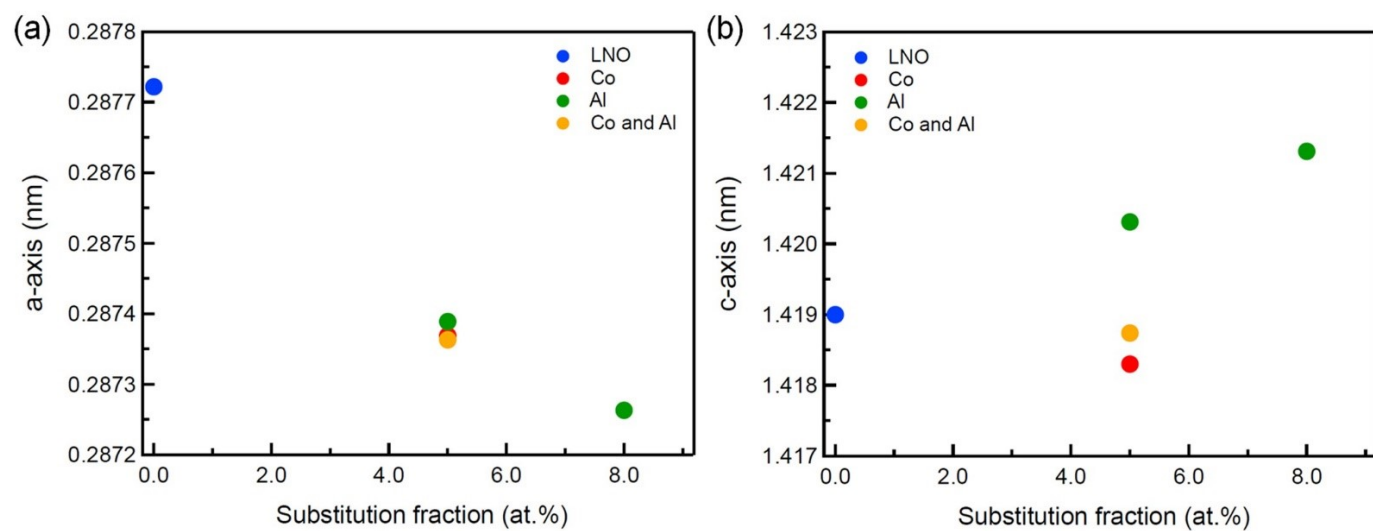


Figure S2 Lattice constant (a) a-axis, (b) c-axis of the prepared samples.

Table S1 Charge-discharge capacity, irreversible capacity loss, and coulombic efficiency of the samples measured in half-cell. The test was conducted in a voltage window of 2.5-4.3 V (cc) at 0.05 C, all at 25°C

Sample	Charge capacity [mAh g ⁻¹]	Discharge capacity [mAh g ⁻¹]	Irreversible capacity loss [mAh g ⁻¹]	Coulombic efficiency [%]
LNO	257	232	25	90.3
NC95	252	238	14	94.4
NA95	251	226	25	90.0
NA92	241	214	27	88.8
NCA95	250	233	17	93.2

Table S2 Discharge capacity of the samples at 0.2 C and 2 C after each cycle

Sample	Discharge capacity after 1 st cycle			Discharge capacity after 300 cycles			Discharge capacity after 500 cycles		
	[mAh g ⁻¹]		2 C/ 0.2 C capacity ratio [%]	[mAh g ⁻¹]		2 C/ 0.2 C capacity ratio [%]	[mAh g ⁻¹]		2 C/ 0.2 C capacity ratio [%]
	0.2 C	2 C		0.2 C	2 C		0.2 C	2 C	
LNO	220	184	83.3	166	106	63.8	150	80	53.3
NC95	222	208	93.6	185	137	73.9	168	112	66.8
NA95	217	197	90.6	177	136	76.9	159	111	70.0
NA92	208	188	90.5	190	162	85.5	174	141	81.0
NCA95	222	206	92.5	189	143	75.6	173	118	68.4

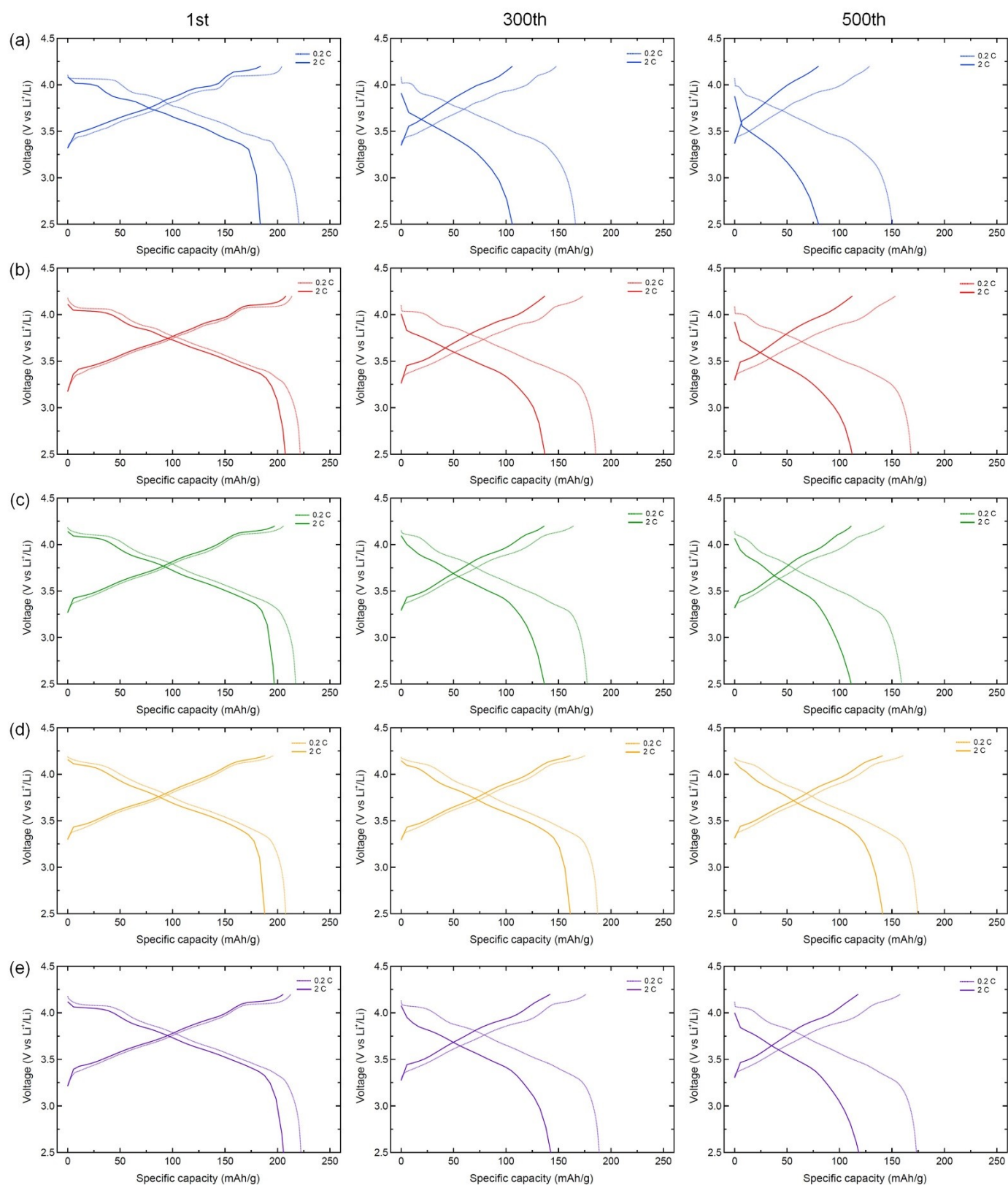


Figure S3 The charge-discharge curve of (a) LNO, (b) NC95, (c) NA95, (d) NA92, (e) NCA95 at 0.2 C (thin) and 2 C (bold) after each cycle.

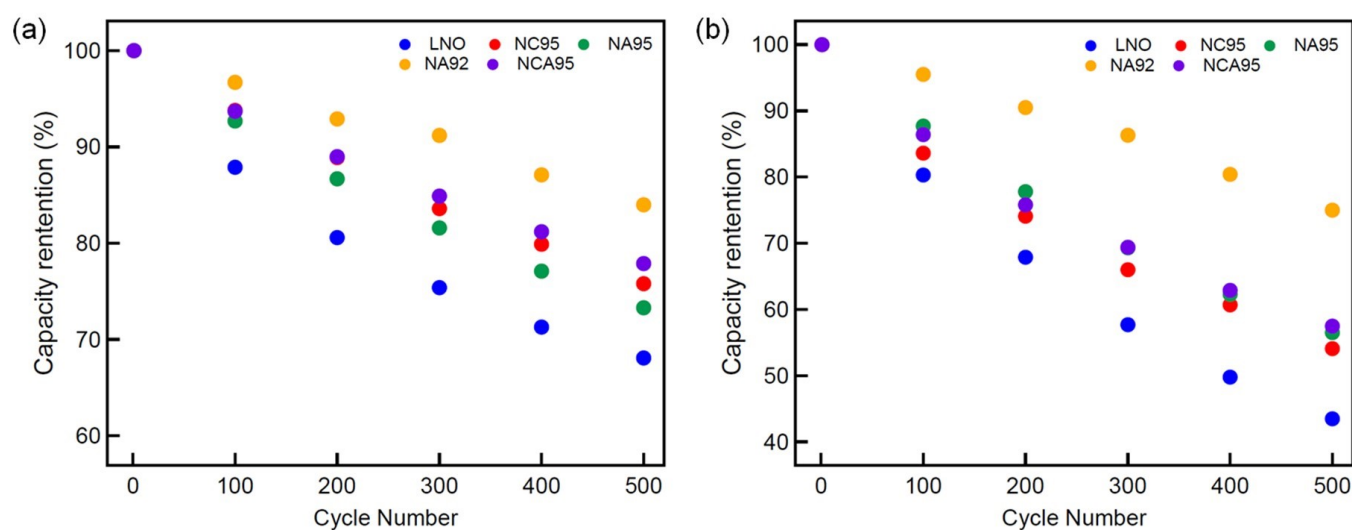


Figure S4 Changes of capacity retention at (a) 0.2 C and (b) 2 C in the samples.

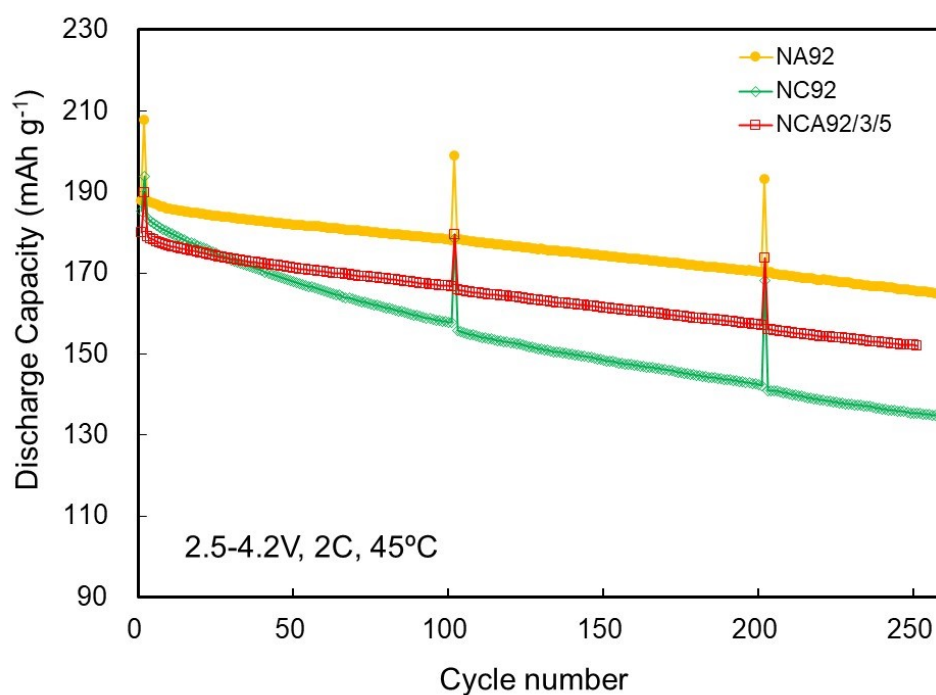


Figure S5 Electrochemical cycling performance of NA92, NC92 and NCA92/3/5 measured in full-cell. The cells were cycled in a voltage window of 2.5-4.2 V at 2 C, all at 45°C. Every 100 cycles were discharged at a 0.2 C rate.

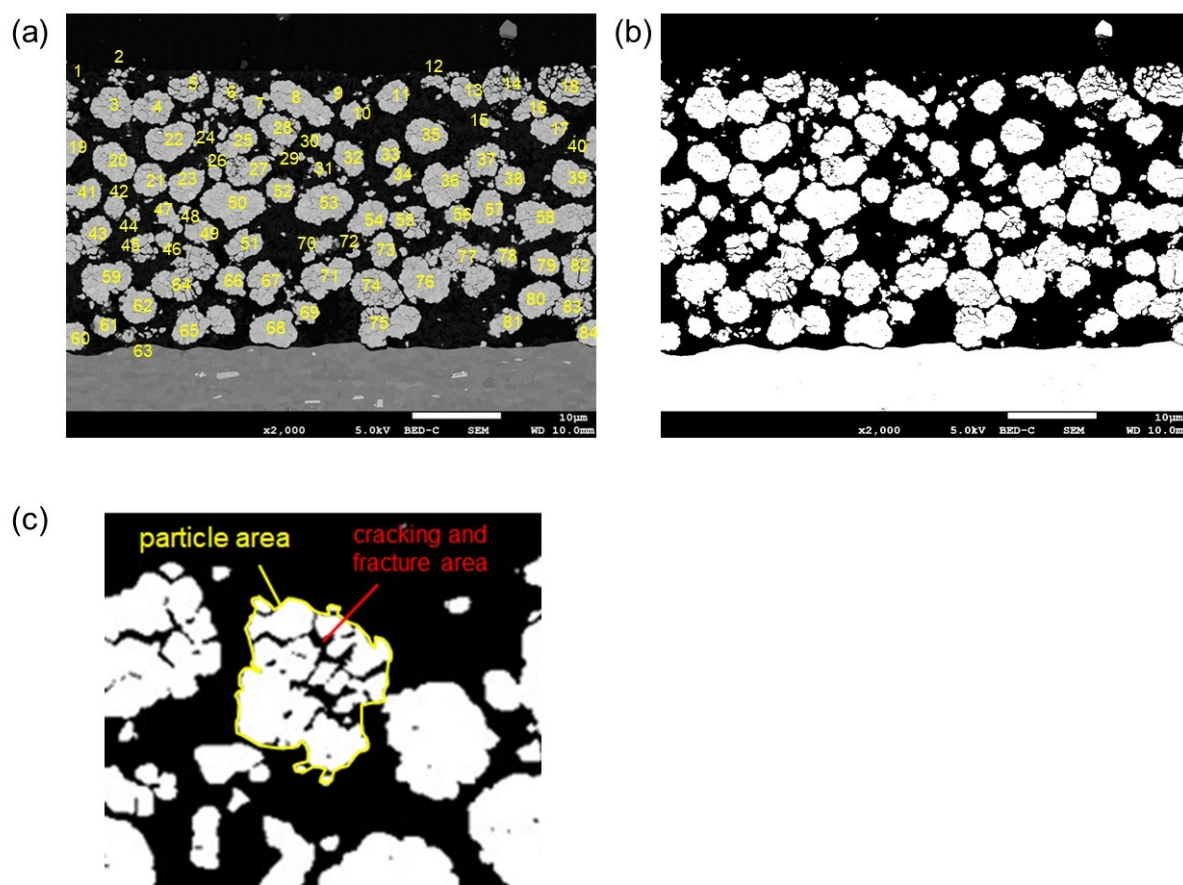


Figure S6 The procedure of quantification for the cracking particles. (a) Numbering of polycrystalline particles (more than 70-80 particles), (b) The image after binarization, (c) The analysis area.

From the cross-sectional SEM image (2k) after the cycle, cracked polycrystalline particles are extracted and numbered like yellow numbers in Fig. S6 (a) (LNO after 500 cycles). Next, ImageJ^[1, 2], an image analysis software, is used to perform binarization. The binarization process is performed automatically (Image → adjust → default → auto). The result of binarization shows in Fig. S6 (b). After the binarization process, the particle area and the cracking and fracture area in the particle were determined for all the numbered particles. As shown Fig. S6 (c), the particle area was defined as the area inside the periphery of the particle (white area surrounded by yellow line), and black area was considered as the area of cracking

and fracture. The degree of particle cracking was obtained by dividing the cracking and fracture area by the particle area.

References

[1] W. S. Rasband, ImageJ, U. S. National Institutes of Health, Bethesda, Maryland, USA, <https://imagej.nih.gov/ij/>, 1997-2018

[2] C. A. Schneider, W. S. Rasband and K. W. Eliceiri, *Nature Methods*, 2012, **9**, 671-675.